UC Irvine
UC Irvine Previously Published Works

Title

Cellular retinoic acid-binding proteins are essential for hindbrain patterning and signal robustness in zebrafish

Permalink

Journal

ISSN

Authors

Cai, Anna Q

Radtke, Kelly

Linville, Angela

et al.

Publication Date

DOI

Copyright Information

Peer reviewed

Cellular retinoic acid-binding proteins are essential for hindbrain patterning and signal robustness in zebrafish

Anna Q. Cai[1,2,3,*], Kelly Radtke[2,4,5,*], Angela Linville[4,5], Arthur D. Lander[2,4,5], Qing Nie[1,2,‡] and Thomas F. Schilling[2,4,5,‡]

SUMMARY

The vitamin A derivative retinoic acid (RA) is a morphogen that patterns the anterior-posterior axis of the vertebrate hindbrain. Cellular retinoic acid-binding proteins (Crabps) transport RA within cells to both its nuclear receptors (RARs) and degrading enzymes (Cyp26s). However, mice lacking Crabps are viable, suggesting that Crabp functions are redundant with those of other fatty acid-binding proteins. Here we show that Crabps in zebrafish are essential for posterior patterning of the hindbrain and that they provide a key feedback mechanism that makes signaling robust as they are able to compensate for changes in RA production. Of the four zebrafish Crabps, Crabp2a is uniquely RA inducible and depletion or overexpression of Crabp2a makes embryos hypersensitive to exogenous RA. Computational models confirm that Crabp2a improves robustness within a narrow concentration range that optimizes a 'robustness index', integrating spatial information along the RA morphogen gradient. Exploration of signaling parameters in our models suggests that the ability of Crabp2a to transport RA to Cyp26 enzymes for degradation is a major factor in promoting robustness. These results demonstrate a previously unrecognized requirement for Crabps in RA signaling and hindbrain development, as well as a novel mechanism for stabilizing morphogen gradients despite genetic or environmental fluctuations in morphogen availability.

KEY WORDS: *Danio rerio*, Hindbrain, Morphogen

INTRODUCTION

Morphogen gradients induce different cell fates depending on concentration. Gradient shape is determined by the source and rate of ligand production, as well as its transport properties and stability (Ben-Zvi and Barkai, 2010; Sample and Shvartsman, 2010; Umulis et al., 2010). Feedback mechanisms such as self-enhanced receptor-mediated degradation also shape morphogen gradients and make them robust (i.e. able to compensate for changes in morphogen availability), as has been demonstrated for growth factors of the TGFβ, Wingless (Wg) and Hedgehog (Hh) families (Eldar et al., 2003; Lander, 2007; Meinhardt, 2009; Wartlick et al., 2009). The vitamin A derivative retinoic acid (RA) determines the identities of hindbrain rhombomeres along the anterior-posterior (A-P) axis (Dupé and Lumsden, 2001; Maves and Kimmel, 2005; White et al., 2007). However, unlike peptide morphogens, RA is hydrophobic and is typically bound to soluble proteins. How these binding proteins function in modulating RA signaling remains unclear.

Cellular RA-binding proteins (Crabps) bind RA with high affinity and solubilize it intracellularly. Vertebrates have two highly conserved Crabps, both of which transport RA to its receptors (RARs) in vitro (Aström et al., 1991; Delva et al., 1999; Budhu et al., 2001; Budhu and Noy, 2002). In addition, Crabp1 protects cells from excess RA by binding it in the cytosol, away from RARs, and

facilitating its degradation by Cyp26s (Boylan and Gudas, 1992; Fiorella and Napoli, 1994; Won et al., 2004). Deletion of both *Crabp1* and *Crabp2* in mice causes supernumerary digits on the forelimb at low penetrance, but adults are otherwise viable (Lampron et al., 1995), suggesting that other proteins can compensate for Crabps in RA signaling (Romand et al., 2000).

RA signaling is also remarkably robust, as might be expected for a signal derived from a dietary precursor. Hindbrain development occurs normally over a ~20-fold range of RA concentrations (Hernandez et al., 2007; White and Schilling, 2008). We previously developed a model explaining how robustness critically depends upon negative feedback, and showed that RA induces expression of the RA-degrading enzyme Cyp26a1 (White et al., 2007). However, our models suggest that self-enhanced degradation alone can only account for a small fraction of the robustness. Crabps might provide additional negative feedback by preventing ligand access to receptors and facilitating degradation (Häcker et al., 2005; Lander et al., 2007).

Here we show that, in contrast to mice, zebrafish Crabp2a and Crabp2b are essential for expression of *hoxb4* and *hoxb5* in the hindbrain. In addition, Crabp2a is uniquely RA inducible and required for robustness. When Crabp2a is depleted or overexpressed, hindbrain patterning becomes hypersensitive to exogenous RA. Computational models with which we simulate the effects of Crabps on gradient robustness indicate that Crabps must be present within a narrow concentration range and must deliver RA both to its receptors and to Cyp26s for degradation.

MATERIALS AND METHODS

Embryo treatments

Wild-type or *Tg(RARE-gata2:NTD-eYFP)Id1* transgenic embryos (Perz-Edwards et al., 2001) were treated with all-trans RA (Sigma) or diethylaminobenzaldehyde (DEAB) as described previously (White et al., 2007). Treatments began at 6 hours postfertilization (hpf) and continued until embryos were fixed in 4% paraformaldehyde (PFA).

[1]Department of Mathematics, University of California Irvine, Irvine, CA 92697, USA. [2]Center for Complex Biological Systems, University of California Irvine, Irvine, CA 92697, USA. [3]School of Mathematics and Statistics, University of New South Wales, Sydney NSW 2052, Australia. [4]Department of Developmental and Cell Biology, University of California Irvine, Irvine, CA 92697, USA. [5]Developmental Biology Center, University of California Irvine, Irvine, CA 92697, USA.

*These authors contributed equally to this work
‡Authors for correspondence (qnie@math.uci.edu; tschilli@uci.edu)

RT-PCR and cloning
RT-PCR was performed with whole-embryo RNA preparations (for primers see supplementary material Table S1). *crabp2a* and *crabp2b* were amplified and cloned into pCS2 (Rupp et al., 1994) for mRNA synthesis.

In situ hybridization
Antisense *crabp2a* and *crabp2b* mRNA probes were synthesized from linearized pCS2 clones (Thisse et al., 2004). Bright-field in situ hybridization and fluorescent images were acquired on a Zeiss Axioplan II compound microscope with Improvision software.

Morpholino (MO) and mRNA injections
One-cell stage embryos were injected with 10 ng Crabp2a-MO1 (CGGG-AATTTTACGATCCATCTTCCG) or 5 ng Crabp2b-MO1 (TGTTTTCT-CCGTGTTAGATTCCATG). Two independent MOs for each gene – Crabp2a-MO2 (TTCTGTCGTTCCTCTGAAAGTAACC) and Crabp2b-MO2 (GTTTCTGCGTGTCTTTCTTTCACTC) – gave similar phenotypes, confirming MO specificity. All MOs were designed to block translation. *crabp2a:mCherry* and *crabp2b:mCherry* constructs were generated by fusion PCR of the *crabp2a* cDNA templates and *mCherry* from a Gateway vector (Invitrogen) (for primers see supplementary material Table S1). Injections were performed with 200 pg *crabp2a:mCherry* or *crabp2b:mCherry* mRNA per embryo, alone or with each MO to confirm MO efficiency. For rescue and overexpression experiments, two full-length crabp2a-pCS2 clones, one with and one without the crabp2a-MO binding sites, were transcribed using SP6 mMessage (Ambion).

Modeling
The model was solved with our newly developed numerical solver (supplementary material Appendices S1, S2), using a scaled domain $x \in [0,1]$ containing the RA gradient between $0 \leq x \leq 0.9$. A domain of Cyp26a1 posterior to $x>0.9$ creates a discontinuity in the gradient. Therefore, $x_{ref}=0.85$ was used and the gradient was modeled between $x=0$ and $x=0.9$. Established biological ranges of parameter values were used or estimated within a realistic range (supplementary material Appendix S3, Tables S2, S3). Exploration of parameter space was performed on a logarithmic scale to include large orders of magnitude. We measured robustness using a probability density distribution $N(E)$, interpreted as the probability of the system producing robustness values in the range $[E_1,E_2]$ with the following formula:

$$\Pr\{E_1 < \overline{E} < E_2\} = \int_{E_1}^{E_2} N(e)\,de . \qquad (1)$$

To ensure that $N(E)$ was representative of the system, we performed consistency checks using increasing numbers of simulations to find the representative distribution. $N(E)$ typically becomes invariant at ~10,000 simulations, but we included many more for higher resolution.

RESULTS AND DISCUSSION
A novel requirement for Crabps in Hox gene expression
Crabps facilitate interactions between RA and RARs in vitro (Aström et al., 1991; Delva et al., 1999; Budhu and Noy, 2002), but also bind RA in the cytosol preventing its entry into the nucleus and promoting degradation (Boylan and Gudas, 1991; Boylan and Gudas, 1992; Fiorella and Napoli, 1994; Chen et al., 2003). Consistent with previous studies (Sharma et al., 2005) of the four zebrafish Crabps (*crabp1a, crabp1b, crabp2a, crabp2b*), all but *crabp1a* were detected during gastrulation (6-9 hpf; supplementary material Figs S1, S2). *crabp2a* and *crabp2b* remained expressed in the presumptive hindbrain at 10-24 hpf. *crabp2a* was expressed in the posterior hindbrain up to rhombomere (R) 4 (supplementary material Fig. S1) and in the anterior spinal cord. *crabp2b* was initially expressed throughout the ectoderm during gastrulation and became progressively restricted to the anterior hindbrain (particularly R2) and somites (supplementary material Fig. S1). These expression patterns suggest overlapping but spatially and temporally distinct roles for each Crabp.

To test functional requirements for Crabps we compared hindbrain patterning in zebrafish embryos injected with antisense morpholino oligonucleotides (MOs) targeting *crabp2a* and *crabp2b*. MOs depleted each target effectively (supplementary material Fig. S3) and specifically, and microinjection of *crabp2a* mRNAs not recognized by MOs targeting their 5′UTRs partially rescued the morphant phenotypes (supplementary material Fig. S4). Embryos injected with either MO alone showed normal patterns of *krox20* (*egr2* – Zebrafish Information Network) (R3, R5) and reduced *hoxb4* (71%, *n*=14) and *hoxb5* (100%, *n*=25) expression in R7 and spinal cord (Fig. 1A-C,I-K). By contrast, embryos co-injected with Crabp2a-MO and Crabp2b-MO completely lacked *hoxb4* (73%, *n*=15; Fig. 1D) and *hoxb5a* (90%, *n*=20; Fig. 1L) expression, suggesting a strong reduction in RA signaling similar to that caused by the loss of *aldh1a2* (Begemann et al., 2001). *hoxb4* expression was not rescued by treatment with 5-20 nM exogenous RA, despite a strong posteriorization of the hindbrain (*n*=14; Fig. 1E-H). Thus, Crabps are required for RA-dependent Hox gene expression in the posterior hindbrain.

Crabp2a is RA inducible and required for signal robustness
Mammalian *Crabp2* contains a retinoic acid response element (RARE) and is RA inducible in vitro (Aström et al., 1994). We examined *crabp2a* and *crabp2b* expression after treatment with RA or an Aldh1a2 inhibitor (DEAB) during gastrulation. Whereas 1 nM RA had no effect on the expression of either gene (data not shown), 10 nM RA induced *crabp2a* expression throughout the CNS (Fig. 2A,B). Conversely, 5 μM DEAB treatments, which phenocopy mutations in *aldh1a2* (Begemann et al., 2001), virtually eliminated *crabp2a* expression (Fig. 2C) but had no effect on *crabp2b* (Fig. 2D-F; supplementary material Fig. S5). Thus, RA is both necessary and sufficient to induce *crabp2a* expression.

To determine the requirements for Crabps in signal robustness, we treated embryos injected with Crabp2a-MO or Crabp2b-MO, or both, during gastrulation with 1-10 nM RA (Fig. 2G-L). Surprisingly, Crabp2a-deficient embryos were ~10-fold more sensitive to exogenous RA than wild-type RA-treated embryos; Crabp2b-MO did not affect RA sensitivity alone or when combined with Crabp2a-MO. Treatment of controls with 1 nM RA caused no hindbrain defects (100%, *n*=22; Fig. 2H), whereas treatment of Crabp2a-MO-injected embryos virtually eliminated the R3 domain of *krox20* and *pax2a* expression at the midbrain-hindbrain boundary (70%, *n*=10; Fig. 2K). Defects resembled those of controls treated with 10-fold higher amounts of RA (100%, *n*=18; Fig. 2I). By contrast, treatments of Crabp2a-deficient embryos with 10 nM RA caused complete loss of *krox20* and anterior expansion of *hoxb4* expression throughout the hindbrain (100%, *n*=8; Fig. 2L). These patterning defects correlate with an expansion of *Tg(RARE-gata2:NTD-eYFP)Id1* transgene expression in Crabp2a-deficient embryos treated with 1 nM exogenous RA (supplementary material Fig. S6) (Linville et al., 2009). Thus, embryos lacking Crabp2a are hypersensitive to small changes in exogenous RA and hindbrain patterning is much less robust.

We also overexpressed Crabp2a and treated embryos with RA or DEAB (Fig. 2M-R). Injection of 50-400 pg *crabp2a* mRNA caused no hindbrain defects (92%, *n*=65; Fig. 2M,P). However, treatment of these embryos with 10 nM RA eliminated *krox20* expression in R3 and both *krox20* and *hoxb4* expression in R5 expanded
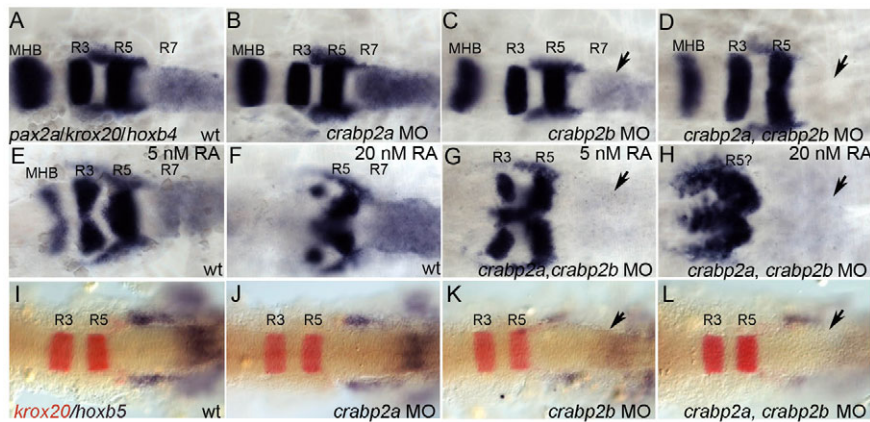
Fig. 1. *crabp2a* and *crabp2b* are required for zebrafish hindbrain patterning. (A-L) Whole-mount in situ hybridization (ISH) for *pax2a* at the midbrain-hindbrain boundary (MHB), *krox20* in rhombomere (R) 3 and R5, and *hoxb4* (A-H) or *hoxb5* (I-L) in R7 and spinal cord at 18 hpf; dorsal views, anterior left. Compared with uninjected controls (A), morpholino (MO) depletion of Crabp2a (B,J) or Crabp2b (C,K) slightly reduces and co-injection (D,L) eliminates *hoxb4* and *hoxb5* expression (arrows). Exogenous RA treatments (5-20 nM) that posteriorize the hindbrain do not rescue *hoxb4* expression (E-H). wt, wild type.

anteriorly (64%, *n*=11; Fig. 2N,Q). Conversely, Crabp2a-overexpressing embryos were less sensitive to 10 μM DEAB (73%, *n*=15; Fig. 2R), which in uninjected embryos eliminated *krox20* expression in R5 and all *hoxb4* expression (89%, *n*=18; Fig. 2O). Thus, excess Crabp2a also reduces robustness.

A computational model predicts crucial roles for Crabps in robustness

Our previous computational model for RA signaling in the zebrafish hindbrain was based on evidence that RA induces (and Fgf inhibits) Cyp26a1 expression, thereby creating a feedback system of RA degradation (White et al., 2007). This system cannot explain the robustness over a 20-fold concentration range observed experimentally (Hernandez et al., 2007; White and Schilling, 2008), suggesting that reversible binding to receptors and binding proteins is crucial. To test this hypothesis, we expanded our model to include equations that model RA interactions with RARs ([R] in models) and Crabps ([BP]) (supplementary material Appendix S1; Fig. 3A). Our model: (1) represents these in a reaction-diffusion system in one spatial dimension (the A-P axis); (2) assumes that extracellular RA diffuses; and (3) is solved at the steady state. The new model captures receptor ($r_{on/off}$) and/or binding protein ($m_{on/off}$) saturation by RA. RA-BP and RA-BP-RAR interactions ($j_{A,B}$) have been demonstrated (Dong et al., 1999), but there is no direct evidence that RA-BP forms a complex with Cyp26, so we used $RAbp_{deg}$ to represent Crabp-assisted RA degradation.

To study robustness characteristics, we sampled randomly generated parameter sets (supplementary material Appendix S1), comparing two values for the RA synthesis rate. We quantified the change in the RA gradient with respect to a fold-change in the RA synthesis of a 'reference' gradient, to define a robustness index designated 'E' (Fig. 3B). E is the normalized mean horizontal shift in two gradients between two thresholds y_1 and y_2 (representing 20% and 80% of the maximum reference value, respectively) when RA synthesis (or any other parameter) is varied. Smaller E values denote higher similarity between the two gradients and therefore a more robust system (Fig. 3C-E). This integrates spatial information across the entire signaling gradient as opposed to quantifying robustness with respect to a threshold value at one location. Parameter space sampling combined with a robustness index dramatically improves comparisons between systems because a representative distribution of *E* values is produced for each one.

To quantify influences of Crabps on RA signal robustness, we first compared a model that contains Crabps with one that does not. E value distributions were determined using ~100,000 simulations of our model for the hindbrain in which the RA synthesis rate was

varied up to 10-fold in each case (Fig. 3F-I; supplementary material Figs S7, S8). For both increases (2-, 5-, 10-fold; Fig. 3F) and decreases (2-, 5-, 10-fold; supplementary material Fig. S9) in RA synthesis, E values were consistently lower in models that included Crabps and showed more simulations with extremely low E values (E=0-0.25) (Fig. 3F-I; supplementary material Fig. S9B-D).

We modeled the effects of varying Crabp levels using randomly generated parameter sets with 5-fold increases or decreases in RA synthesis rate and simulated for 20 different Crabp synthesis rates
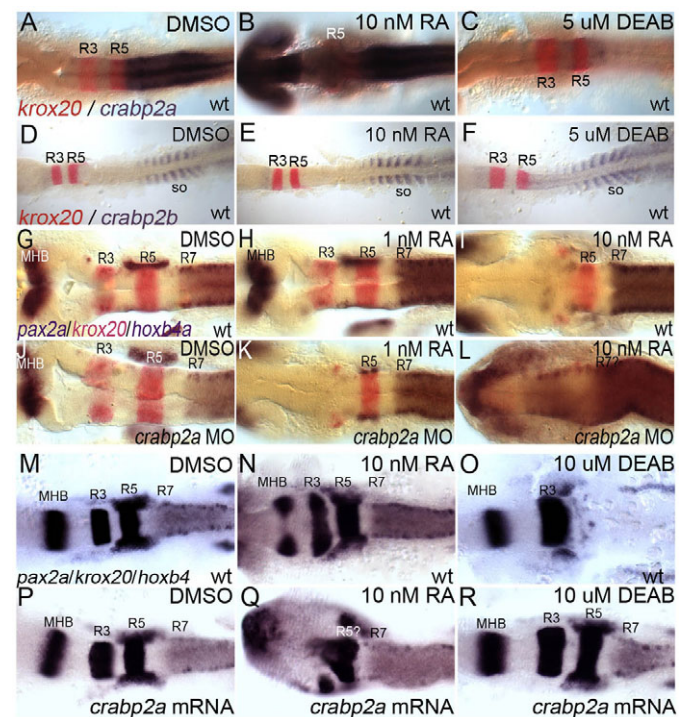
Fig. 2. *crabp2a* is RA inducible and required for signal robustness. (A-F) Whole-mount ISH for *crabp2a/b* expression at 15 hpf; dorsal views, anterior left. *crabp2a* (A-C) is expressed posterior to the R5/6 boundary, whereas *crabp2b* (D-F) expression is restricted to somites. Treatment with 10 nM RA expands *crabp2a* expression anteriorly throughout the CNS (B) but has no effect on *crabp2b* (E). Treatment with 5 μM DEAB eliminates *crabp2a* expression (C) but does not disrupt *crabp2b* (F). **(G-R)** *pax2a*, *krox20* and *hoxb4* expression at 18 hpf in uninjected controls (G-I), Crabp2a-MO-injected (J-L) and *crabp2a* mRNA-injected embryos (M-R) treated with 1 nM RA (H,K), 10 nM RA (I,L,N,Q) or 10 μM DEAB (O,R). so, somites.

Fig. 3. Computational models indicate essential roles for Crabps in robustness. (**A**) Schematic of RA signaling in one cell illustrating model components: RA (red), Crabps (purple crescents), Cyp26s associated with endoplasmic reticulum (ER, blue), RA-degradation products ([deg], red dots). Green arrows indicate components induced by RA and red inhibitory symbols indicate components repressed by RA. (**B**) A robustness index (E) utilized:

$$E = \frac{1}{x(y_1)} \sqrt{\frac{1}{y_2 - y_1} \int_{y_1}^{y_2} \Delta x^2 \, dy}, \quad y_1 = 0.2(y_{ref} - y_{min}) + y_{min}, \quad y_2 = 0.8(y_{ref} - y_{min}) + y_{min}, \tag{2}$$

where y_{min} is the minimum value and $y_{ref}(x_{ref})$ is an imposed maximum value of the reference gradient. (**C-E**) Three examples of calculated gradients very similar (C) or different (D,E) from the reference gradient (red line) across the hindbrain primordium (x-axis) and corresponding E values. (**F-I**) Probability density distributions (percentages, y-axis) of E values (x-axis) for models tha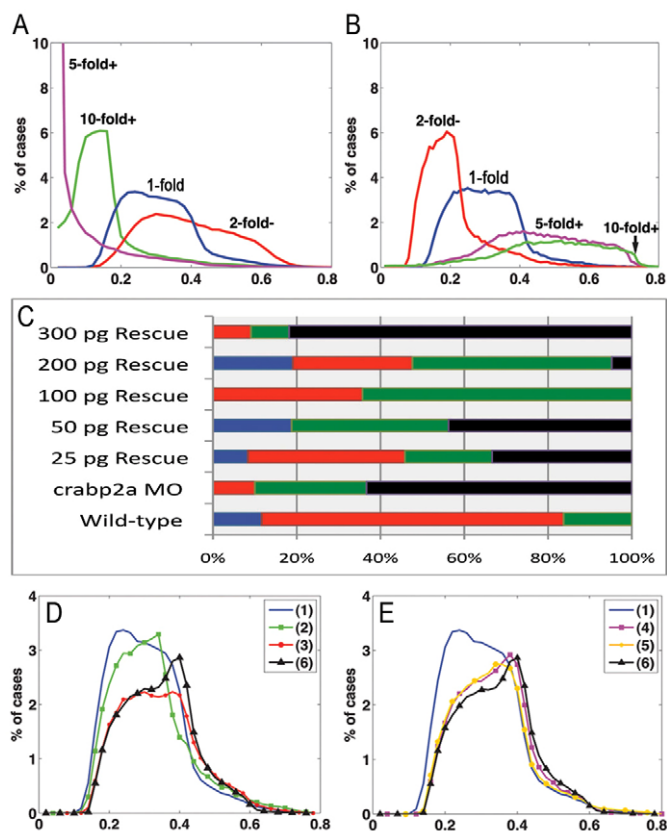t either include binding proteins (solid lines) or do not (dashed lines) for models with a 2-fold (black lines, G), 5-fold (blue lines, H) or 10-fold (red lines, I) increase in [RA]$_{out}$ synthesis rate.

[V$_{bp}$] (supplementary material Fig. S10). Synthesis rates were obtained by logarithmically dividing its parameter range (supplementary material Appendix S3). The lowest E values corresponded to an intermediate level of V$_{bp}$ in both cases. This suggests an optimal range of Crabp concentration, above or below which robustness is compromised. To examine this in more detail, E value distributions were generated for simulations with a 5-fold increase in RA synthesis rate coupled with either a 5- or 10-fold increase or a 2-fold decrease in the Crabp synthesis rate V$_{bp}$ (Fig. 4A). E value distributions were lowest with a 5-fold increase in V$_{bp}$, with many E values close to zero (Fig. 4A). Similarly, E value distributions for simulations with a 5-fold decrease in RA synthesis rate were lower when V$_{bp}$ was increased (Fig. 4B; supplementary material Fig. S11). These simulations show that proportional changes in Crabp and RA synthesis produce the best robustness.

Based on these models, we tested the concentration range over which Crabp2a promotes optimal robustness in the hindbrain experimentally, by co-injecting Crabp2a-MO with a range of doses of *crabp2a* 'rescue' mRNA and treating the embryos with 5 nM exogenous RA. This relatively low amount of RA reduces *krox20* expression in R3 in wild types (mild), whereas in Crabp2a-depleted embryos R3 expression is lost and R5 is reduced (severe). Co-injection of 100-200 pg/embryo *crabp2a* mRNA partially rescued these phenotypes, whereas 25-50 pg had little effect and higher amounts (>300 pg) increased the severity of the phenotype (Fig. 4C; supplementary material Fig. S4).

Models suggest that Crabps facilitate RA degradation

Crabp2 in mice has a putative nuclear localization signal and can form a complex with RA and RARs, while Crabp1 enhances the formation of RA degradation products in vitro (Dong et al., 1999). Although our model does not distinguish between different Crabps, it can address questions regarding how positive or negative roles influence gradient robustness. We hypothesize three such roles: (1) Crabps transport RA to receptors, j_A in our models (Fig. 3A); (2)

Fig. 4. Robustness gains require Crabp-mediated RA degradation.
(**A**,**B**) E value distributions for models with either a 5-fold increase (A) or
decrease (B) of RA synthesis rate with respect to 10- (green), 5-
(magenta), or 2-fold (red) increases in V_{bp}. (**C**) Percentages (x-axis) of
wild-type (blue bars), mild (red bars), moderate (green bars) and severe
(black bars) phenotypes resulting from injection of different amounts of
Crabp2a mRNA per embryo (y-axis) treated with 5 nM RA.
(**D**,**E**) Simulations of 5-fold increases in RA synthesis rate in which
binding proteins: (1) have all three mechanisms; (2) do not transport RA
to receptors (j_B=0); (3) do not sequester RA (j_A=0); (4) do not transport
RA to Cyp26 degradation ($rabp_{deg}$=0); (5) must bind RA to allow
degradation (ra_{deg}=0); and (6) are absent.

Crabps bind RA and prevent interactions with receptors, j_A=0
sequestering RA as [RA-BP] and allowing less [RA-R]
(supplementary material Figs S12, S13); and (3) Crabps transport
RA for degradation by Cyp26s. These roles are not mutually
exclusive.

To test each role computationally, we calculated E values for
models incorporating different combinations (Fig. 4D,E): (1) all
three functions; (2) only sequestration and degradation; (3)
transport to receptors and degradation; (4) transport to receptors
and sequestration; (5) degradation only when bound to RA
(RA_{deg}=0); and (6) no binding proteins present. Simulations with
either 5-fold increases (Fig. 4D,E) or decreases (supplementary
material Fig. S14) in RA synthesis rate revealed that combined
positive and negative roles were most robust, particularly a model
incorporating all three roles. By contrast, a system without
sequestration was least robust. The receptor/sequestration model
(Fig. 4E) was less robust than the dual sequestration/degradation
model, suggesting that transport to Cyp26s is crucial for robustness
in the RA system.

These results are consistent with Crabps both facilitating
interactions between RA and RARs and promoting RA degradation
(Fig. 3A) (Dong et al., 1999). They help explain how hindbrain
patterning can be robust to a 20-fold range of RA concentrations
(Hernandez et al., 2007). They also reveal an essential role for
these proteins that can help explain why Crabps are so highly
conserved – zebrafish Crabp2a is 74% similar in protein sequence
to human CRABP2 (Sharma et al., 2003). The apparent lack of a
requirement for Crabps in mice might reflect differential
redundancies among fatty acid-binding proteins or differential
regulation in placental mammals at the level of maternal and extra-
embryonic tissues (Sapin et al., 1997; Zheng and Ong, 1998).

Competing interests statement
The authors declare no competing financial interests.

Supplementary material
Supplementary material available online at
http://dev.biologists.org/lookup/suppl/doi:10.1242/dev.077065/-/DC1

References
Allenby, G., Janocha, R., Kazmer, S., Speck, J., Grippo, J. F. and Levin, A. A.
(1994). Binding of 9-cis-retinoic acid and all-trans-retinoic acid to retinoic acid
receptors alpha, beta, and gamma. Retinoic acid receptor gamma binds all-
trans-retinoic acid preferentially over 9-cis-retinoic acid. *J. Biol. Chem.* **269**,
16689-16695.
**Aström, A., Tavakkol, A., Pettersson, U., Cromie, M., Elder, J. T. and
Voorhees, J. J.** (1991). Molecular cloning of two human cellular retinoic acid-
binding proteins (CRABP). Retinoic acid-induced expression of CRABP-II but not
CRABP-I in adult human skin in vivo and in skin fibroblasts in vitro. *J. Biol. Chem.*
266, 17662-17666.
Aström, A., Pettersson, U., Chambon, P. and Voorhees, J. J. (1994). Retinoic
acid induction of human cellular retinoic acid-binding protein-II gene
transcription is mediated by retinoic acid receptor-retinoid X receptor
heterodimers bound to one far upstream retinoic acid-responsive element with
5-base pair spacing. *J. Biol. Chem.* **269**, 22334-22339.
Begemann, G., Schilling, T. F., Rauch, G. J., Geisler, R. and Ingham, P. W.
(2001). The zebrafish neckless mutation reveals a requirement for raldh2 in
mesodermal signals that pattern the hindbrain. *Development* **128**, 3081-3094.
Ben-Zvi, D. and Barkai, N. (2010). Scaling of morphogen gradients by an
expansion-repression integral feedback control. *Proc. Natl. Acad. Sci. USA* **107**,
6924-6929.
Boylan, J. F. and Gudas, L. J. (1991). Overexpression of the cellular retinoic acid
binding protein-I (CRABP-I) results in a reduction in differentiation-specific gene
expression in F9 teratocarcinoma cells. *J. Cell Biol.* **112**, 965-979.
Boylan, J. F. and Gudas, L. J. (1992). The level of CRABP-I expression influences
the amounts and types of all-trans-retinoic acid metabolites in F9
teratocarcinoma stem cells. *J. Biol. Chem.* **267**, 21486-21491.
Budhu, A., Gillilan, R. and Noy, N. (2001). Localization of the RAR interaction
domain of cellular retinoic acid binding protein-II. *J. Mol. Biol.* **305**, 939-949.
Budhu, A. S. and Noy, N. (2002). Direct channeling of retinoic acid between
cellular retinoic acid-binding protein II and retinoic acid receptor sensitizes
mammary carcinoma cells to retinoic acid-induced growth arrest. *Mol. Cell. Biol.*
22, 2632-2641.
Chen, A. C., Yu, K., Lane, M. A. and Gudas, L. J. (2003). Homozygous deletion
of the CRABPI gene in AB1 embryonic stem cells results in increased CRABPII
gene expression and decreased intracellular retinoic acid concentration. *Arch.
Biochem. Biophys.* **411**, 159-173.
**Delva, L., Bastie, J. N., Rochette-Egly, C., Kraïba, R., Balitrand, N., Despouy,
G., Chambon, P. and Chomienne, C.** (1999). Physical and functional
interactions between cellular retinoic acid binding protein II and the retinoic
acid-dependent nuclear complex. *Mol. Cell. Biol.* **19**, 7158-7167.
Dong, D., Ruuska, S. E., Levinthal, D. J. and Noy, N. (1999). Distinct roles for
cellular retinoic acid-binding proteins I and II in regulating signaling by retinoic
acid. *J. Biol. Chem.* **274**, 23695-23698.

Dupé, V. and Lumsden, A. (2001). Hindbrain patterning involves graded responses to retinoic acid signalling. *Development* **128**, 2199-2208.

Eldar, A., Rosin, D., Shilo, B. Z. and Barkai, N. (2003). Self-enhanced ligand degradation underlies robustness of morphogen gradients. *Dev. Cell* **5**, 635-646.

Fiorella, P. D. and Napoli, J. L. (1994). Microsomal retinoic acid metabolism. Effects of cellular retinoic acid-binding protein (type I) and C18-hydroxylation as an initial step. *J. Biol. Chem.* **269**, 10538-10544.

Häcker, U., Nybakken, K. and Perrimon, N. (2005). Heparan sulphate proteoglycans: the sweet side of development. *Nat. Rev. Mol. Cell Biol.* **6**, 530-541.

Hernandez, R. E., Putzke, A. P., Myers, J. P., Margaretha, L. and Moens, C. B. (2007). Cyp26 enzymes generate the retinoic acid response pattern necessary for hindbrain development. *Development* **134**, 177-187.

Lampron, C., Rochette-Egly, C., Gorry, P., Dollé, P., Mark, M., Lufkin, T., LeMeur, M. and Chambon, P. (1995). Mice deficient in cellular retinoic acid binding protein II (CRABPII) or in both CRABPI and CRABPII are essentially normal. *Development* **121**, 539-548.

Lander, A. D. (2007). Morpheus unbound: reimagining the morphogen gradient. *Cell* **128**, 245-256.

Lander, A. D., Nie, Q. and Wan, F. Y. (2007). Membrane-associated non-receptors and morphogen gradients. *Bull. Math. Biol.* **69**, 33-54.

Linville, A., Radtke, K., Waxman, J. S., Yelon, D. and Schilling, T. F. (2009). Combinatorial roles for zebrafish retinoic acid receptors in the hindbrain and pharyngeal arches. *Dev. Biol.* **325**, 60-70.

Maves, L. and Kimmel, C. B. (2005). Dynamic and sequential patterning of the zebrafish posterior hindbrain by retinoic acid. *Dev. Biol.* **285**, 593-605.

Meinhardt, H. (2009). Models for the generation and interpretation of gradients. *Cold Spring Harb. Perspect. Biol.* **1**, a001362.

Napoli, J. L. (1996). Biochemical pathways of retinoid transport, metabolism, and signal transduction. *Clin. Immunol. Immunopathol.* **80**, S52-S62.

Perz-Edwards, A., Hardison, N. L. and Linney, E. (2001). Retinoic acid-mediated gene expression in transgenic reporter zebrafish. *Dev. Biol.* **229**, 89-101.

Romand, R., Sapin, V., Ghyselinck, N. B., Avan, P., Le Calvez, S., Dollé, P., Chambon, P. and Mark, M. (2000). Spatio-temporal distribution of cellular retinoid binding protein gene transcripts in the developing and the adult cochlea. Morphological and functional consequences in CRABP- and CRBPI-null mutant mice. *Eur. J. Neurosci.* **12**, 2793-2804.

Rupp, R. A., Snider, L. and Weintraub, H. (1994). *Xenopus* embryos regulate the nuclear localization of XMyoD. *Genes Dev.* **8**, 1311-1323.

Sample, C. and Shvartsman, S. Y. (2010). Multiscale modeling of diffusion in the early Drosophila embryo. *Proc. Natl. Acad. Sci. USA* **107**, 10092-10096.

Sapin, V., Ward, S. J., Bronner, S., Chambon, P. and Dollé, P. (1997). Differential expression of transcripts encoding retinoid binding proteins and retinoic acid receptors during placentation of the mouse. *Dev. Dyn.* **208**, 199-210.

Sharma, M. K., Denovan-Wright, E. M., Boudreau, M. E. and Wright, J. M. (2003). A cellular retinoic acid-binding protein from zebrafish (Danio rerio): cDNA sequence, phylogenetic analysis, mRNA expression, and gene linkage mapping. *Gene* **311**, 119-128.

Sharma, M. K., Saxena, V., Liu, R. Z., Thisse, C., Thisse, B., Denovan-Wright, E. M. and Wright, J. M. (2005). Differential expression of the duplicated cellular retinoic acid-binding protein 2 genes (crabp2a and crabp2b) during zebrafish embryonic development. *Gene Expr. Patterns* **5**, 371-379.

Thisse, B., Heyer, V., Lux, A., Alunni, V., Degrave, A., Seiliez, I., Kirchner, J., Parkhill, J. P. and Thisse, C. (2004). Spatial and temporal expression of the zebrafish genome by large-scale in situ hybridization screening. *Methods Cell Biol.* **77**, 505-519.

Umulis, D. M., Shimmi, O., O'Connor, M. B. and Othmer, H. G. (2010). Organism-scale modeling of early Drosophila patterning via bone morphogenetic proteins. *Dev. Cell* **18**, 260-274.

Wartlick, O., Kicheva, A. and González-Gaitán, M. (2009). Morphogen gradient formation. *Cold Spring Harb. Perspect. Biol.* **1**, a001255.

White, R. J. and Schilling, T. F. (2008). How degrading: Cyp26s in hindbrain development. *Dev. Dyn.* **237**, 2775-2790.

White, R. J., Nie, Q., Lander, A. D. and Schilling, T. F. (2007). Complex regulation of cyp26a1 creates a robust retinoic acid gradient in the zebrafish embryo. *PLoS Biol.* **5**, e304.

Won, J. Y., Nam, E. C., Yoo, S. J., Kwon, H. J., Um, S. J., Han, H. S., Kim, S. H., Byun, Y. and Kim, S. Y. (2004). The effect of cellular retinoic acid binding protein-I expression on the CYP26-mediated catabolism of all-trans retinoic acid and cell proliferation in head and neck squamous cell carcinoma. *Metabolism* **53**, 1007-1012.

Zheng, W. L. and Ong, D. E. (1998). Spatial and temporal patterns of expression of cellular retinol-binding protein and cellular retinoic acid-binding proteins in rat uterus during early pregnancy. *Biol. Reprod.* **58**, 963-970.

DEVELOPMENT